UNIVERSITÀ DEGLI STUDI DI PADOVA

Thermal Design and Performance Analysis of a High Heat-Flux Condensation System

Author:

Kaleb Kassa Lafebo

kalebkassa.lafebo@studenti.unipd.it

Corresponding Professor

Professor Andrea Diani

Table of Contents

Table of Figures:

List of Tables:

Abstract

This report presents the design of a horizontal shell-and-tube condenser for the complete condensation of water vapor entering at 0.010627 MPa and 60°C, transferring 43 kW of thermal energy to cooling water at 33°C. The design leverages copper tubes for high thermal conductivity and corrosion resistance, arranged in a triangular pitch configuration to optimize heat transfer. Key thermal and mechanical parameters were calculated, including the log mean temperature difference, shell-side and tube-side heat transfer coefficients, and pressure drops using the *Kern method* and *Lockhart-Martinelli correlations*.

The final design features *40 tubes* of *12.7 mm* outer diameter and *3.08 m* total length, enclosed by a *173.7 mm* diameter shell. *While the condenser meets the thermal duty, the shell-side pressure drop approaches the limit for vacuum operation, suggesting future optimization through increased shell diameter or double-segmental baffles.* This project highlights the integration of thermodynamic principles, iterative mechanical design, and collaborative problem-solving to achieve an efficient and feasible heat exchanger.

Introduction

Heat exchangers are fundamental components in thermal energy systems, this project focuses on designing a horizontal shell-and-tube condenser to fully condense water vapor at 0.010627 MPa and 60°C while transferring 43 kW to cooling water. The heat released during condensation, amounting to 43 kW, is transferred to cooling water entering the system at an initial temperature of 33 °C.

Objective and scope.

The primary objective of this project is to design a shell-and-tube heat exchanger capable of condensing superheated water vapor at 60 °C and 0.010627 MPa by transferring 43 kW of thermal energy to subcooled water entering at 33 °C. The design focuses on selecting appropriate geometric configurations and thermal parameters to ensure efficient condensation under low-pressure conditions.

The scope of the project includes:

- Selection of a suitable heat exchanger type based on thermodynamic requirements.
- Design of the heat exchanger layout, including shell and tube arrangement, material, and flow configuration.
- Use of computational tools such as Microsoft Excel and Python to perform thermal and hydraulic calculations.
- Generation of illustrative diagrams and simplified models to support conceptual understanding.
- Justification of design choices based on efficiency, feasibility, and industry best practices.

This project does not include CFD or experimental validation but rather emphasizes a rigorous theoretical and computational approach to the design process.

Heat Exchanger Selection.

Considering the inlet vapor pressure of 0.010627 MPa and referring to the design guidelines provided by L. Rossetto et al [1]. a horizontal shell-and-tube condenser with condensation occurring on the shell side (outside the tubes) is well-suited for applications involving pressures below 0.04 MPa. Given these conditions, a shell-and-tube heat exchanger was selected due to its proven effectiveness and thermal efficiency in handling phase change processes, particularly condensation. The horizontal orientation enhances condensate drainage and heat transfer performance, making it an optimal configuration for the specified operating conditions.

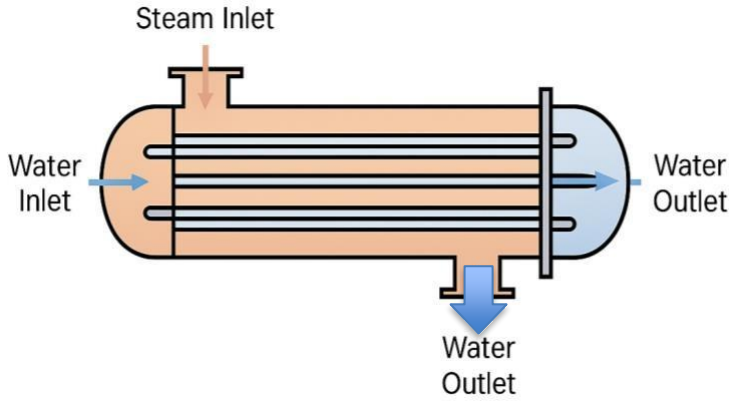

Figure 1: General Shell and Tube layout.

Working Fluids

Water is used as the working fluid on both sides of the heat exchanger (*Figure 1*). On the tube side, subcooled liquid water enters at a temperature below its saturation point and acts as the cooling medium. On the shell side, superheated steam is introduced, with an inlet temperature of 60 °C, significantly above the saturation temperature of 47 °C at 0.010627 MPa. As the steam comes into contact with the cooler tube surfaces, it condenses by releasing latent heat to the water flowing inside the tubes.

Methodology (Calculations)

Assumptions

1. **Thermal Assumptions:**
   - **Saturation Temperature $T_{sat} = 47°C$** at 0.010627 MPa obtained from REFPROP.

   Based on the provided data and using REFPROP, we assumed a condensation temperature of **47 °C** for the water vapor. This value was determined by referencing the saturation temperature corresponding to the given inlet vapor pressure. This assumption serves as a basis for the subsequent energy balance and heat transfer calculations.

   - **Outlet temperature** of the cooling fluid is assumed following the simplified method for a Counterflow Heat exchanger (Case 3), referring to the L. Rossetto et al [1].

   $$\Delta T = T_{sat} - T_{w,out} = 5°C$$
   $$T_{w,out} = 42°C$$

   Since we have $T_{sat} > T_{w,out}$ and $\Delta T = 5K$ we will have only **Sensible + Latent** heat exchange process.
   - Wall temperature: For the first iteration, it is considered that $T_{wall} = T_{w,out} = 42$
   - **Correction Factor (Ft = 1)** - Isothermal phase change process. Therefore, when condensing pure vapor, the temperature profile remains constant, and there is no need for LMTD correction.
2. **Fluid Property Assumptions:**
   - Thermophysical Properties are constant (Thermophysical properties obtained from REFPROP are constant)
3. **Mechanical Design Assumptions:**
   - **Tube arrangement:** A 30° triangular tube arrangement was considered, given its compactness, and the pitch ratio is taken as Triangular Pitch (Pt/de = 1.4).
   -

4. **Other assumptions:**
   - Operation is a Steady state.
   - Heat losses are negligible: Heat losses from the system are considered negligible due to the implementation of standard thermal insulation around the shell. This effectively creates an adiabatic boundary, with the surrounding

Input Data and Thermophysical properties from REFPROP

- Input Data from the design problem and other thermal data, after assumptions are obtained from REFPROP and listed below in Table 1.

Vapor pressure at the inlet	$P_{v,\text{in}}$	0.010627	MPa
Vapor temperature at the inlet	$T_{v,\text{in}}$	60	°C
Heat flow rate transferred	$\dot{Q}$	43	kW
Water temperature at the inlet	$T_{w,\text{in}}$	33	°C
Water temperature at the outlet	$T_{w,\text{out}}$	42	°C
Vapor Saturation Temperature	T_{sat}	47	°C

Table 1: Input fluid properties and other thermal data after the initial assumptions (REFPROP)

- Properties of Condensing Steam

For vapor at saturation temperature, constant and equal $T_{sat} = 47°C$

For liquid at the mean temperature of the film

$$T_{mean,film} = \frac{T_{sat} + T_{wall}}{2} = 44.5°C$$

Latent heat r [kJ/kg]	Liquid density ρ_L[kg/m³]	Vapor density ρ_V[kg/m³]	Liquid viscosity μ_L [kg/ms]	Thermal conductivity of liquid λ_L [W/mK]
2389.2	990.38	0.0722	0.00060108	0.63413

Table 2: Thermophysical properties from REFPROP. (Liquid properties at mean film temperature and the vapor properties at saturation temperature)

- Properties of Cooling Water

Liquid water properties are taken at the mean temperature between the inlet and outlet of the cooling water. (37.5 °C)

$$T_{w,\text{mean}} = \frac{T_{w,\text{in}} + T_{w,\text{out}}}{2} = \frac{33 + 42}{2} = 37.5°C$$

.

Specific heat Cp_w[kJ/kgK]	Density ρ_w[kg/m³]	Viscosity μ_w [kg/ms]	Thermal conductivity λ_w [W/mK]
4.1795	993.11	$0.68 * 10^{-6}$	0.62511

Table 3: Thermophysical properties of water from REFPROP

Log mean temperature difference

To calculate LMTD, we again recall the simplified model for crossflow counter current (Case 3), referring to the L. Rossetto et al [1].

LMTD represents an average temperature driving force for heat transfer between the two fluids and allows us to accurately evaluate the thermal performance of the system.

Case – 3: Simplified Method: Valid if the outlet temperature of the cooling fluid < saturation temperature of the condensing fluid (Saturation temperature of the condensing fluid - outlet temperature of the cooling fluid) > 4 - 5 K

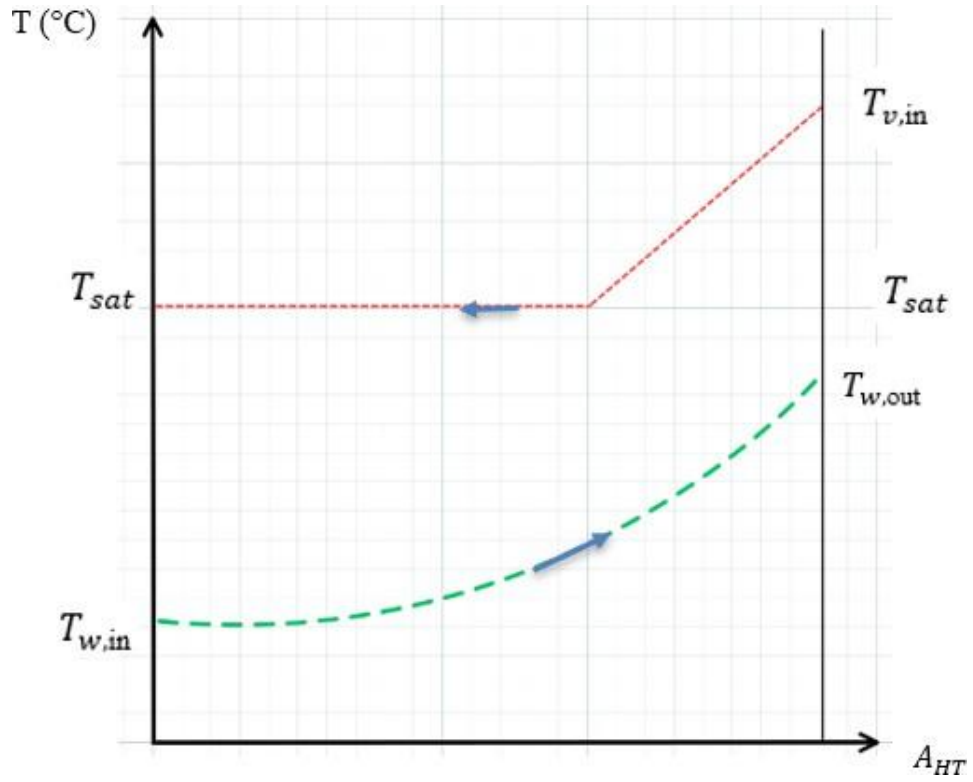

Figure 2: Crossflow configuration for Simplified case

Thus, LMTD will be given by:

$$\Delta T_{lm} = \frac{\Delta_1 - \Delta_2}{\ln\left(\frac{\Delta_1}{\Delta_2}\right)}$$

where:

$$\Delta_1 = T_{sat} - T_{w,out}$$

$$\Delta_2 = T_{sat} - T_{w,in}$$

$$\Delta T_{lm} = \frac{\Delta_1 - \Delta_2}{\ln\left(\frac{\Delta_1}{\Delta_2}\right)} = \frac{5 - 14}{\ln\left(\frac{5}{14}\right)} = 8.74109°C$$

$$Q = q_{sensible} + q_{latent} = \Delta T_{lm} . A_{HT} . K_e$$

Since the steam undergoes isothermal condensation, the correction factor Ft, which is a parameter to adjust the ideal **log mean temperature difference (LMTD)** to account for the actual temperature distribution caused by the flow arrangement, is assumed equal to 1.

Initial heat transfer coefficient

We needed to estimate the overall heat transfer coefficient Ke, which represents the total resistance to heat transfer through the heat exchanger walls and includes contributions from convection on both fluid sides and conduction through the wall. It is a key parameter that influences the heat transfer rate between the two fluids.

To estimate this value, we referred to a specific table (Appendix 1) provided in the textbook "Trasmissione del calore" by Bonacina, as recommended by the professor. Based on the fluids involved in our system—water on one side and a light organic vapor condensing on the other—we selected an overall heat transfer coefficient of:

$$K_{e,first\ try} = 1000\ \mathrm{W/m^2}$$

Tubes selection

For the tube material of the heat exchanger, we made technical considerations based on thermal performance, corrosion resistance, and mechanical strength. After evaluating several options, we selected **copper** as the most suitable material.

Copper offers **excellent thermal conductivity**, which significantly enhances the overall heat transfer rate. This property is especially important in heat exchangers, where efficient energy transfer between fluids is critical. Additionally, copper has good **corrosion resistance** in water and many organic fluids, ensuring long-term durability and reduced maintenance.

Its **workability** and **ease of fabrication** also make it advantageous for manufacturing, especially for tubes that may require bending or precise dimensions. While copper may be more expensive than some alternative metals, its superior heat transfer characteristics justify its use in applications where performance is a priority.

- **Thermal conductivity**

To evaluate the thermal conductivity of the material, we used the following table:

Industrial material	Copper	Alluminum	Admiralty alloy	Cu-Ni 90-10	Cu-Ni 70-30	Carbon steel	Inox steel	Titanium
$\lambda(Wm^{-1}K^{-1})$	310	180	120	65	40	38	18	18

Table 4: Estimated values of the thermal conductivity

Therefore, the thermal conductivity of copper will be:

$$\lambda_{Cu} = 310\ W/(m \cdot K)$$

- **Allowable velocities**

From the textbook, we obtained the **minimum and maximum allowable velocities** for the fluid inside the tube. These reference values help ensure proper flow conditions, avoiding excessive pressure drops at high velocities and poor heat transfer at low velocities.

In the case of **copper tubes**, the recommended velocity range is:

$$u_{min} = 1.2\ m/s$$

$$u_{max} = 1.8\ m/s$$

We fixed our velocity at $u = 1.5\ m/s$

These values were used as design constraints in our analysis.

- **Diameters and thickness**

Regarding the **tube dimensions**, we referred to the Anglo-Saxon standard (Appendix 2). Based on our design requirements and standard conformity, we selected a tube with the following external diameter and wall thickness.

$$d_e = 12.7\ mm$$

$$\delta = 1.245\ mm$$

From these values, we calculated the **internal diameter** as:

$$d_i = d_e - 2\,\delta = 12.7 - 2 \cdot 1.245 = 10.21\ mm$$

- **Mass flow rate calculations**

The mass flow rate of the condensing steam and the cooling water per condenser unit are computed through the standard heat transfer equation for sensible heat:

$$Q = m_w \cdot c_p \cdot (T_{w,out} - T_{w,in})$$

So, for water side:

$$m_w = \frac{Q}{cp.\Delta T} = \frac{43000}{4179.5 \cdot (42 - 33)} = \frac{43000}{37615.5} = 1.1431\ kg/s$$

While, for the vapor side we used the latent heat equation:

$$Q = m_v \cdot r$$

$$m_w = \frac{Q}{r} = \frac{43000}{2389200} = 0.018\ kg/s$$

Geometry of the heat exchanger

Based on the operating pressure and design requirements, we chose to design a **shell-and-tube heat exchanger** with **horizontal tubes**, where condensation occurs **outside the tubes**, in the shell side. This configuration is well-suited for handling condensation of vapor at moderate pressures (<0.04 MPa) and allows for efficient heat transfer and ease of maintenance.

Tube Geometry

To determine the required number of tubes, we first calculated the total **cross-sectional flow area** needed for the water side using the following equation:

$$S_i = m_{water}/(\rho_{water} \cdot u_{water})$$

Substituting the values:

$$S_i = \frac{1.14314}{993.11 \cdot 1.5} = 0.0007674\ m^2$$

- **Number of tubes for one passage**

Next, we computed the number of **tubes per pass** using the internal diameter of the tubes:

$$N_{t,1pass} = \frac{4 \cdot Si}{\pi \cdot 0.01021^2} = 9.38$$

So, we approximate to the nearest largest whole number, **10**.

- **Length of tubes**

Starting from the heat transfer equation that includes the correction factor and the overall heat transfer coefficient, we calculated the total heat exchange area required:

$$Q = K_e \cdot A \cdot \Delta T_{lm} \cdot Ft$$

We obtained the total required heat transfer area:

$$A = \frac{Q}{K_e \cdot \Delta T_{ml} \cdot Ft} = \frac{4300}{1000 \cdot 8.74109 \cdot 1} = 4.91929\ m^2$$

Having determined the total surface area and knowing the **total number of tubes** and the **external diameter** of each tube, we calculated the required **tube length**:

$$L = \frac{A}{N_{tt} \cdot \pi \cdot d_e}$$

No. of passes	*Total number of tubes*	*Tube length (m)*
1	10	12.329603
2	20	6.164801
4	40	3.082401
6	60	2.054934
8	80	1.541200

Table 5: Length for different numbers of passes.

The relationship between the number of passes, total tubes, and tube length demonstrates a critical design trade-off in the heat exchanger configuration. As shown in the plot, increasing the number of passes from 1 to 4 reduces the required tube length significantly (from ~12.3 m to 3.08 m) while proportionally increasing the total tube count (from 10 to 40 tubes). This occurs because additional passes enhance fluid velocity and turbulence, improving the heat transfer coefficient and allowing shorter tubes to achieve the same thermal duty. However, beyond 4 passes, the pressure drop rises sharply without substantial gains in compactness.

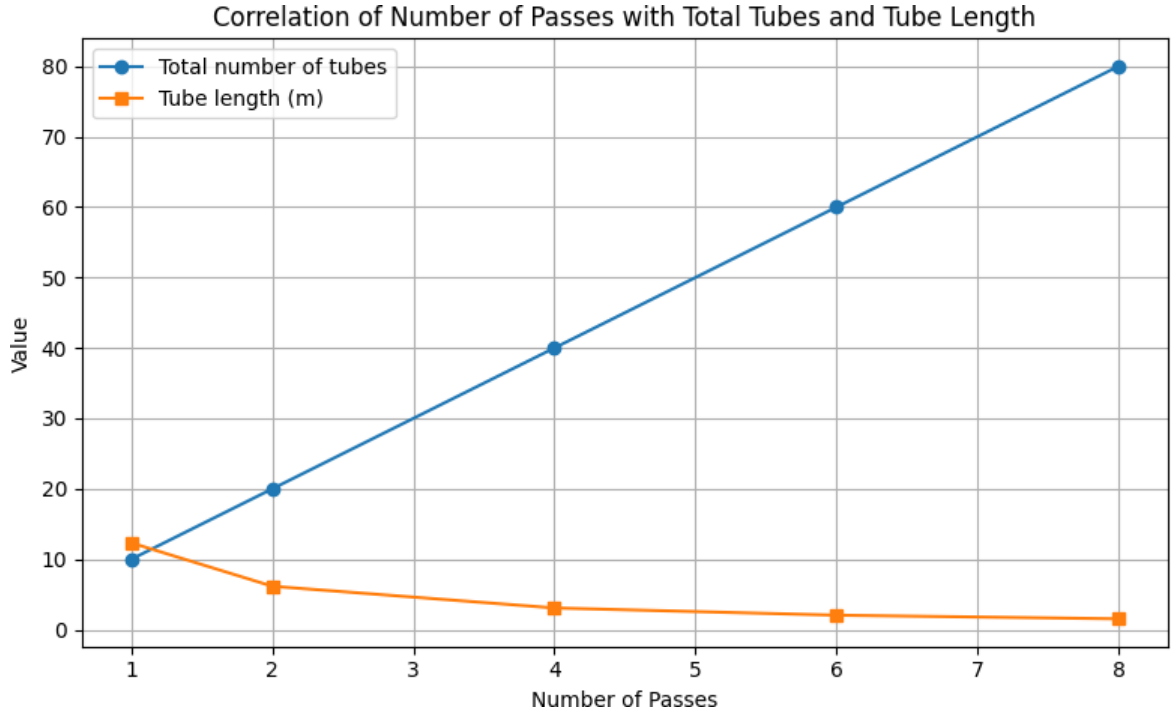

Figure 3: Correlation between the total number of tubes, the tube length, and the number of passes.

The ***4-pass*** configuration was selected as optimal because it balances thermal performance (maintaining Re > 10,000 for turbulent flow) with practical constraints—achieving the target heat transfer area (4.92 m²) with manageable ΔP while fitting standard shell diameters. This aligns with Kern's recommended velocity range (1.5 m/s)

- **Number of passages**

To ensure the desired level of turbulence while avoiding excessive pressure drop, we selected:

$$N_{pass} = 4$$

- **Number of tubes**

Finally, the **total number of tubes** is calculated as:

$$N_{tt} = N_{t,1pass} \cdot N_{pass} = 10 \cdot 4 = 40\ tubes$$

- **Effective velocity**

The actual velocity of the fluid in the tubes can be evaluated

$$u_i = \frac{4mN_{PASS}}{\rho\pi d_i^{\,2} N_{tt}} = \frac{4 \cdot 1.143 \cdot 4}{993.11 \cdot \pi \cdot 10.21^2 \cdot 40} = 1.41\ m/s \approx 1.5\ m/s$$

- **Tube pitch calculation**

For the tube layout, we selected a triangular pitch configuration, meaning the tubes are arranged at a 30° angle. This design was chosen to maximize the heat exchanger's efficiency, as it promotes better fluid distribution and facilitates cleaning and maintenance.

To determine the appropriate tube pitch distance between the centers of two adjacent tubes, we referred to standard design guidelines. According to these, the pitch should satisfy the condition:

$$1.25 < \frac{pt}{d_e} < 1.5$$

To remain near the average of this recommended range, we multiplied the external diameter of the tube by **1.4**, resulting in:

$$pt = 1.4 \cdot 12.7 = 17.78\ mm$$

This pitch ensures an optimal balance between compactness and sufficient spacing for heat transfer and mechanical stability.

Shell sizing

- **Iterative computation of D_{ct}**

To estimate the tube bundle diameter (diameter of the circumference passing through the centers of the external tubes), we started from the general design equation used to calculate the initial number of tubes:

$$N_{tt} = \frac{\pi \cdot {D_{ct}}^2}{4 \cdot C_1 \cdot pt^2}$$

- C1= 0.866 suggested for triangular tube layout θ=30°C

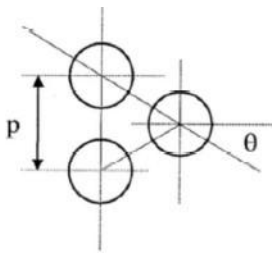

This equation gives an initial estimation of the number of tubes in the bundle. However, to refine the value of D_{ct} We also used the correction factor Φ, which accounts for the incomplete circular packing of tubes:

$$N_{tt} = (1 - \phi) \cdot N_{tt,initial}$$

The correction factor Φ is a function of the ratio:

$$\phi = f(\frac{D_{ct}}{p_t})$$

We began with an assumed value of D_{ct}, calculated with ϕ=0. Then we calculated the corresponding Φ using standard design graphs. Since we obtained an initial value of 118.11 mm, we could not retrieve the value of Φ directly from the graph (Figure 4). We extrapolate the value on the interval of our interest with an extrapolation graph, considering our case of 4 passages.

Extrapolation Procedure: considering our number of passes 4, we collect Φ value by extending the curve horizontally for every available D_{ct} value, refer to (Figure 4)

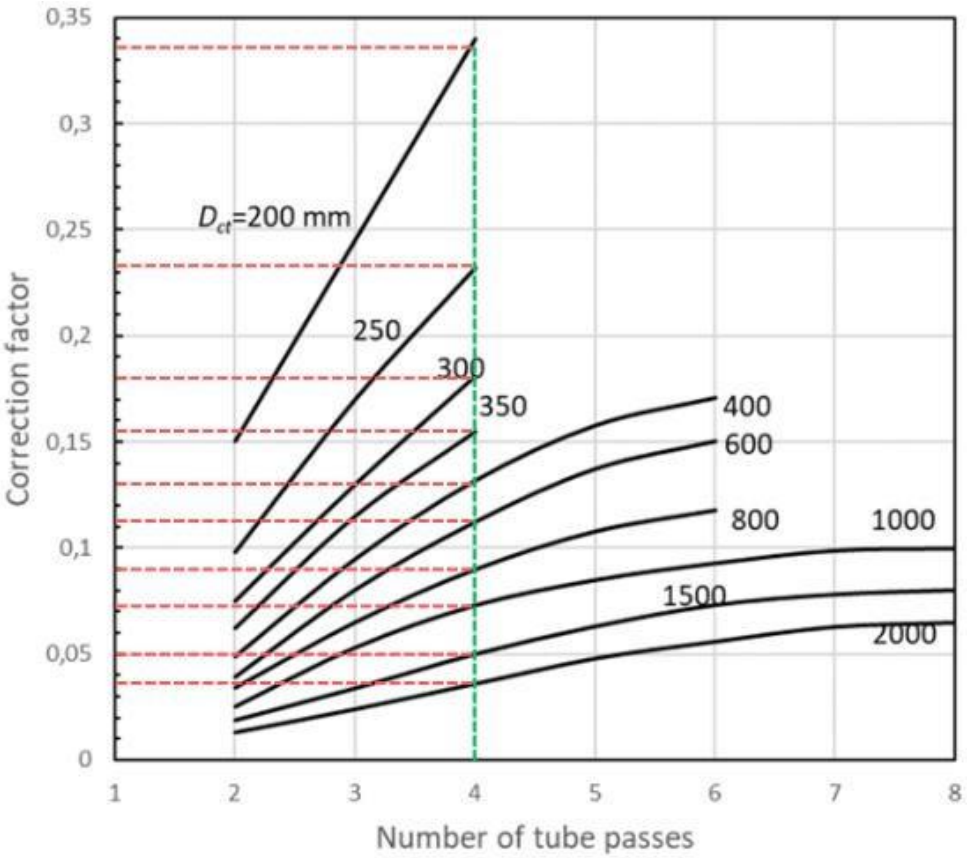

Figure 4: Extrapolating the correlation.

Then we separately plot Φ vs D_{ct} curve to recognize the pattern, to visualize the convergence of the D_{ct} values, and by doing so, accurately estimate the final D_{ct}.

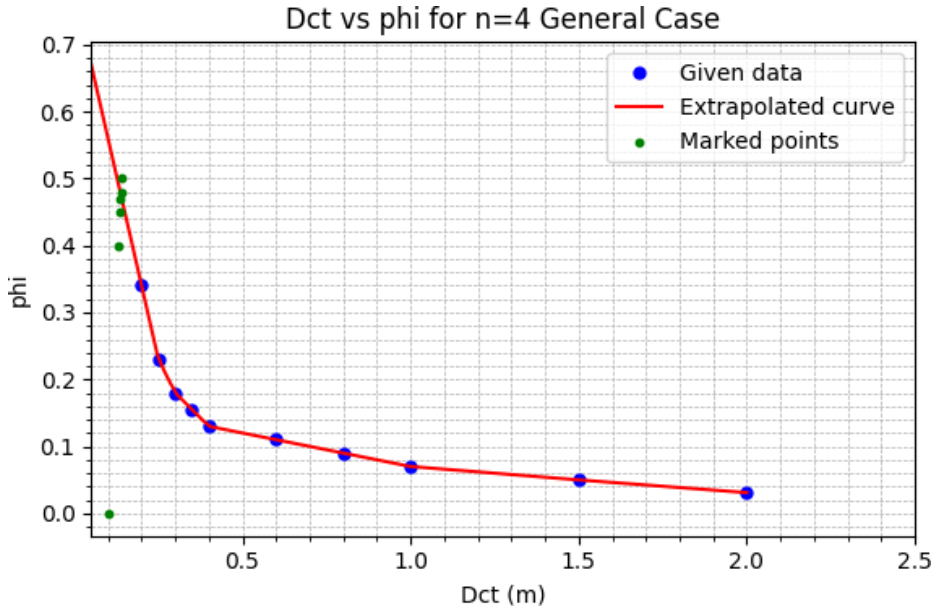

Figure 5: Extrapolation curve.

The green dots refer to each iteration of the D_{ct} and the corresponding Φ value. As the green dots close to each other, while lying on the red curve (extrapolation curve), the value of D_{ct} will converge

Through **iterative refinement**, adjusting both Φ and D_{ct} We converged to a final value of:

Iterative approach: $$D_{ct} = (Ntt \cdot 4 \cdot C_1 \cdot pt^2/(\pi \cdot (1 - \phi))^{0.5}$$

D_{ct} [mm] Initial	ϕ	D_{ct}[mm] final
	0	118.11
118.11	0.46	160.73
160.73	0.34	145.38
145.38	0.36	147.64
147.64	0.37	148.80
148.80	0.38	149.99

Table c: Dct Iteration result.

Therefore the D_{ct} will converge to $D_{ct} = 149\ mm$

- **Bundle diameter Df**

The final bundle diameter is calculated as the sum of the tube cluster diameter and one external tube diameter, to account for the outermost tube layer:

$$Df = Dct + de = 149 + 12.7 = 161.7\ mm$$

This value represents the total diameter occupied by the tube bundle inside the shell and is essential for defining the shell size.

- **Shell-to-bundle clearance L_{fm}**

In addition to the bundle diameter, it is necessary to include the clearance between the tube bundle and the **shell wall**, known as the **bundle-to-shell clearance**. This value ensures proper shell-side flow distribution and allows for thermal expansion and mechanical tolerances.

Based on the design graph provided below

Considering a Fixed tube sheet, we selected:

$$L_{fm} = 12\ mm$$

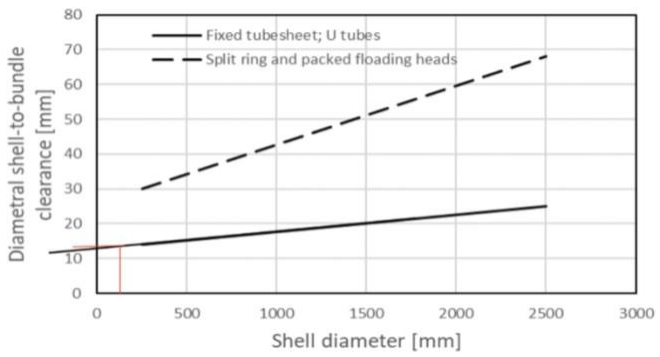

Figure c: Correlation between Shell-tube clearance and the shell diameter.

Therefore, the shell diameter is calculated by adding this clearance to the final bundle diameter:

$$Dm = Df + Lfm = 161.7 + 12 = 173.7\ mm$$

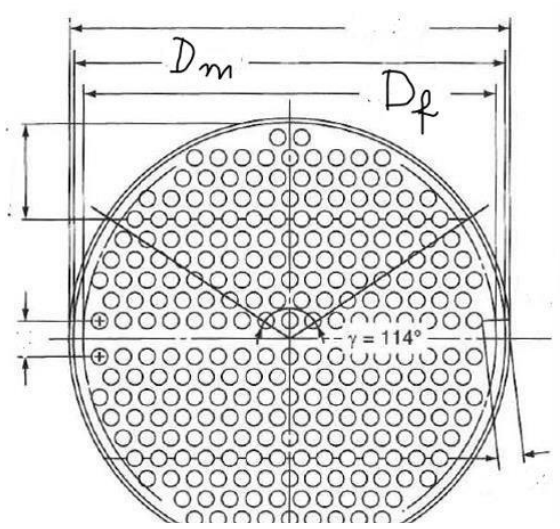

Figure 7: Cross-section of Shell and tube condenser.

Heat transfer coefficient calculations

Heat transfer coefficient, tube side

On the tube side, we have a flow of liquid water. The heat transfer coefficient is retrieved from the Dittus-Boelter equation.

$$Nu = 0.023 \cdot Re^{0.8} \cdot Pr^{0.33}$$

$$Nu = \frac{\alpha \cdot di}{\lambda}$$

$$\alpha = \frac{\lambda_w \cdot 0.023 \cdot Re_w^{0.8} \cdot Pr_w^{0.33}}{di}$$

- $\lambda_w = 0.62511\ W/m^2$
- $\rho_w = 993.11\ kg/m^3$
- $\mu_w = 0.00068461\ Pa \cdot s$
- $di = 10.21\ mm$
- $u_w = 1.41\ m/s$
- $Re_w = (\rho_w \cdot u_w \cdot di)/\mu_w = (993.11 \cdot 1.41 \cdot 10.21)/0.00068461 = 20833.54 > 10000$
- $Pr_w = (cp_w \cdot \mu_w)/\lambda_w = (4.18 \cdot 0.000685)/0.625 = 4.58$

$$\alpha = (0.62511 \cdot 0.023 \cdot 20833.54^{0.8} \cdot 4.58^{0.33})/10.21 = 6632.40\ W/m^2 \cdot K$$

Heat transfer coefficient, shell side

On the shell side, there is vapor condensing on the external surface of horizontal tubes. Gravity-driven condensation governs the heat transfer process. We can evaluate the heat transfer coefficient with Nusselt's theory.

Condensation on a single horizontal tube

The average heat transfer coefficient on a horizontal tube is:

$$\alpha_1 = 0.725[(\lambda_L{}^3 \cdot g \cdot \rho_L \cdot (\rho_L - \rho_V) \cdot r)/(\mu_L \cdot D \cdot (t_s - t_P)]^{1/4}$$

L: properties of the liquid phase (condensed)

V: properties of the vapor phase

$\lambda_L = 0.63413\ W/m^2$
$\rho_L = 990.38\ kg/m^3$
$\rho_V = 0.0722\ kg/m^3$
$\mu_L = 0.00060108\ Pa \cdot s$
$r = 2389.2\ kJ/kg$
$ts = 47\ °C$
$t_P = 42°C$
$D = 12.7\ mm$

$$\alpha_1 = 0.725[(0.63413 \cdot 9.81 \cdot 990.38 \cdot (990.38 - 0.0722) \cdot 2389.2)/(0.00060108 \cdot 12.7 \cdot (47 - 42)]^{1/4}$$

$$\alpha_1 = 14352.2\ W/m^2 \cdot K$$

Condensation on a tube row

In horizontal shell tube heat transfer, there is a vertical column of tubes; the condensate from the upper tube drips onto the tube below, forming a thicker liquid film. This reduces the thermal resistance as it enhances the resistance.

$$\alpha_N = \alpha_1 \cdot N^{-1/6}$$

N is the number of tubes stacked vertically in the shell

$$N = 2/3 \cdot (Dct/(pt \cdot C_1 \cdot 2) = 2/3 \cdot (149/17.78 \cdot 0.866 \cdot 2) = 3.23$$

$$N = 4$$

$$\alpha_N = 14352.2 \cdot 4^{-1/6} = 11391.35\ W/m^2 \cdot K$$

Overall heat transfer coefficient

To evaluate the thermal performance of the condenser, the effective overall heat transfer coefficient $K_{e,real}$ is determined. This coefficient incorporates all significant resistances to heat flow, including convective heat transfer on both the shell and tube sides, fouling factors that account for surface impurities or deposits, and the conduction resistance through the tube wall. The fouling factor was retrieved from (Appendix 1) provided in the textbook "Trasmissione del calore" by Bonacina. By considering these parameters, a more realistic and comprehensive assessment of the condenser's heat transfer efficiency is achieved.

$$K_{e,real} = \frac{1}{\frac{d_e}{\alpha'_w d_i} + f_{si} \cdot \frac{d_e}{d_i} + f_{se} + \frac{d_e \ln(\frac{d_e}{d_i})}{2\lambda_{tube}} + \frac{1}{\alpha'_N}}$$

$$K_{e,real} = \frac{1}{\frac{0.0127}{0.01021 \cdot 6632.40} + 0.00017 \cdot \frac{0.0127}{0.01021} + 0 + \frac{d_e \ln\left(\frac{0.0127}{0.01021}\right)}{2 \cdot 310} + \frac{1}{11391.35}}$$

$$K_{e,real} = 2046.11\ W/(m^2 \cdot K)$$

- **Verify the Assumption**

Initial assumption: $\Delta T_{assumed} = T_{sat} - T_{wall} = 5°C \quad , \quad T_{wall} = 42°C$

Verification: $\Delta T_{new} = T_{sat} - T_{wall} = (K_{e,real} \cdot \Delta T_{lm} \cdot F_t)/\alpha'_N$

$$= 2046.11 \cdot 8.74109°C \cdot \frac{1}{11391.35} = 1.57°C$$

$$\Delta T_{assumed} \neq \Delta T_{new} \qquad , \quad T_{wall} = 45.43°C$$

Hence, further Iteration is required, considering the new T_{wall} to retrieve thermophysical properties from REFPROP.

- **New Area and length.**

Considering the new overall heat transfer coefficient:

$$A_{e,real} = \frac{Q}{K_{e,real} \cdot \Delta T_{ml} \cdot Ft} = \frac{4300}{2046.11 \cdot 8.74109 \cdot 1} = 2.40\ m^2$$

$$L_{1,tube} = \frac{A_{e,real}}{N_{tt} \cdot \pi \cdot d_e} = \frac{2.40}{4 \cdot \pi \cdot 0.0127} = 1.51\ m$$

Iteration 2:

For the second iteration, we consider the new wall temperature to get the Thermophysical properties from REFPROP.

For vapor at saturation temperature, constant and equal $T_{sat} = 47°C$

For liquid at the mean temperature of the film

$$T_{mean,film} = \frac{T_{sat} \pm T_{wall}}{2} = 46.215°C$$

Latent heat r [kJ/kg]	Liquid density ρ_L[kg/m³]	Vapor density ρ_V[kg/m³]	Liquid viscosity μ_L [kg/ms]	Thermal conductivity of liquid λ_L [W/mK]
2391.2	989.69	0.0722	0.00058323	0.63612

Table 7: Thermophysical properties at the new mean film temperature for the liquid and saturation temperature for the vapor

Summary table

Same calculation were done with the new thermophysical properties of the mean film temperature of the liquid

Table 8: Second iteration results

$K_{e,real}\ [W/(m^2 \cdot K)]$	$A_{e,real}\ [m]^2$	$L_{1,tube}\ [m]$	ΔT_{new} [°C]
2049.59	2.40	1.51	1.56

Baffle spacing and mechanical support

The use of baffles inside the shell is necessary to provide mechanical support and enhance cross-flow tube bundle. To define the spacing we referred to standard guidelines:

$$1.25 < \frac{q}{Dm} < 1.5$$

To remain near the average of this recommended range, we multiplied the inner diameter of the tube by **0.6**, resulting in:

$$q = 0.6 \cdot 173.7 = 104.22\ mm$$

$$q_{in} = q_{out} = 0.8 \cdot 173.7 = 138.96\ mm$$

The maximum supported length of a tube depends on the tube material group and outer diameter. Since we are using copper, which belongs to material group B and $6 \leq de \leq 19\ mm$

$$L_{b,max} = 60 \cdot de + 177 = 60 \cdot 12.7 + 177 = 939\ mm$$

According to mechanical standard, we must ensure:

$$2q < L_{b,max}\ , \quad q_{in} + q < L_{b,max}, \quad q_{out} + q < L_{b,max}$$

With our values:

$$2q\ =\ 2{\cdot}104.22\ =\ 208.44\ mm$$

$$q_{in} + q = 138.96 + 138.96 = 277.92\ mm$$

Since all values are lower than $L_{b,max} = 939\ mm$, the design satisfied mechanical support requirement.

Number of baffles: 4

Pressure drops

In this section, the pressure drops across both the shell and tube sides of the condenser is evaluated. On the tube side, where liquid water circulates, a more significant pressure drop is expected and will be calculated using established engineering equations. Conversely, on the shell side, where steam condenses and its density increases markedly, the pressure loss is generally minimal. However, for accuracy, it will also be quantified using appropriate and validated empirical correlations.

Pressure drops on the tube side

The total pressure drops along the tube side is composed of two main components:

$$-\Delta p_{tot} = \Delta p_f \pm \Delta p_{conc}$$

The **distributed pressure drop** Δp_f is calculated using the Darcy-Weisbach equation:

$$-\Delta p_f = \frac{2fL\rho_w u^2{}_w}{d_i}$$

- $f = 0.079\, Re_w^{-0.25} = 0.079\,(20833.54)^{-0,25} = 0{,}006576$ friction factor
- $L = 4 \cdot L_{tube} = 4 \cdot 1.51\ m = 6.0187\ m$
- $\rho_w = 993.11\ kg/m^3$
- $u_w = 1.41\ m/s$
- $d_i = 10.21\ mm$

so, the distributed pressure drops are:

$$-\Delta p_f = -(2 \cdot 0.006576 \cdot 6.0187\ m \cdot 993.11\ kg/m^3 \cdot (1.41\ m/s)^2)/10.21\ mm$$
$$= -15233.73\ Pa$$

The **concentrated pressure drops**, due to localized effects such as the one at the inlet and at the outlet (expansion and contraction), is calculated as follows:

$$-\Delta_{conc} = -4 \cdot ((4\rho_w u^2{}_w)/2)$$
$$-\Delta p_{conc} = -4 \cdot ((4 \cdot 993.11 \cdot (1.41)^2/2) = -15720.04\ Pa$$

Total pressure drop. Summing both main contributions

$$-\Delta p_{tot} = -\Delta p_f \pm \Delta p_{conc} = -15233.73 - 15720.04 = -30953.77 Pa =$$
$$\Delta p_{tot} = 0.310\ bar$$
$$0.310\ bar < 2\ bar$$

The total pressure drop is within the acceptable range for tube-side pressure drops in an industrial condenser (2 bar), confirming the hydraulic feasibility of the design.

Pressure drops shell side

On the shell side, superheated vapor undergoes complete condensation. To evaluate the associated pressure drop, the Kern method for single-phase flow was applied. The analysis was conducted separately for the vapor and liquid phases, allowing for a comparative assessment of the pressure losses in each state.

Kern equation considering if there was only vapor

The **distributed pressure drops**

$$-\Delta p_{distributed} = 0.5\, f\, (L_k/D_k)(\rho_{vapor} u^2{}_k)(\mu/\mu_P)^{-0.14}$$

The parameters are:

- $D_k = 4(0.866p^2 - \pi de^2/4)/(\pi de) = 4(0.866 \cdot 17.78 - \pi \cdot 12.7^2/4)/(\pi \cdot 12.7) = 14.76\ mm$
- $L_k = (nbaffles + 1) \cdot D_m = (4 + 1) \cdot 173.3 = 868.5mm$
- $A_k = ((p - d_e) \cdot q \cdot D_m)/p = ((17.78 - 12.7) \cdot 104.22 \cdot 173.7)/17.78 = 5172.29\ mm^2$
- $u_k = m_{vap}/(\rho_{vapor} \cdot A_k) = 0.0180/(0.0722 \cdot 5172.29) = 48.2\ m/s$
- $Re_k = D_k u_k \rho_{vapor}/\mu_{vapor} = 14.76 \cdot 48.2 \cdot 0.0722/0.000010416 = 4930.97 > 300$
- $f = 1.76 Re_k^{-0.19} = 1.76 \cdot 4930.97^{-0.19} = 0.35$
- $\mu_p = 0.00059124\ Pa \cdot s$ found with Refprof

$$-\Delta p_{distributed} = -0.5 \cdot 0.35 \cdot (868.5/14.76)(0.0722 \cdot 48.2^2)\left(\frac{0.000010416}{0.00059124}\right)^{-0.14} =$$

$$\Delta p_{distributed} = 3038.04\ Pa$$

The **concentrated pressure drops** are:

$$-\Delta P_{conc} = -4 \cdot ((4\rho_{vapor} u^2{}_k)/2)$$

$$-\Delta p_{conc} = -4 \cdot ((4 \cdot\ 0.0722 \cdot (48.2)^2)/2) = -1341.60\ Pa$$

$$\Delta p_{conc} = 1341.60\ Pa$$

Total pressure drops. Summing both main contributions

$$-\Delta p_{tot} = -\Delta p_f + -\Delta p_{conc} = -3038.04 - 1341.59 = -4379.62\ Pa$$

$$\Delta p_{tot} = 4.37kPa$$

Kern equation considering if there was only liquid

The **distributed pressure drops**

$$-\Delta p_{distributed} = 0.5\ f\ (L_k/D_k)(\rho_{cond} u^2{}_k)(\mu/\mu_P)^{-0.14}$$

The parameters are:

- $D_k = 4(0.866p^2 - \pi de^2/4)/(\pi de) = 4(0.866 \cdot 17.78 - \pi \cdot 12.7^2/4)/(\pi \cdot 12.7) = 14.76\ mm$
- $L_k = (nbaffles + 1) \cdot D_m = (4 + 1) \cdot 173.3 = 868.5mm$
- $A_k = ((p - d_e) \cdot q \cdot D_m)/p = ((17.78 - 12.7) \cdot 104.22 \cdot 173.7)/17.78 = 5172.29\ mm^2$
- $u_k = m_{cond}/(\rho_{cond} \cdot A_k) = 0.0178/(989.69 \cdot 5172.29\ ) = 0.0035\ m/s$
- $Re_k = D_k u_k \rho_{cond}/\mu_{cond} = 14.76 \cdot 0.0035 \cdot 989.69/0.0005838 = 87.98 < 300$
- $f = 1$ found from the graph
- $\mu_p = 0.00059124\ Pa \cdot s$ retrieved from REFPROP

- $-\Delta p_{distributed} = -0.5 \cdot 1 \cdot (868.5/14.76)(989.69 \cdot 48.2^2)(0.0005838/0.00059124)^{-0.14} =$

$$\Delta p_{distributed} = 0.361\ Pa$$

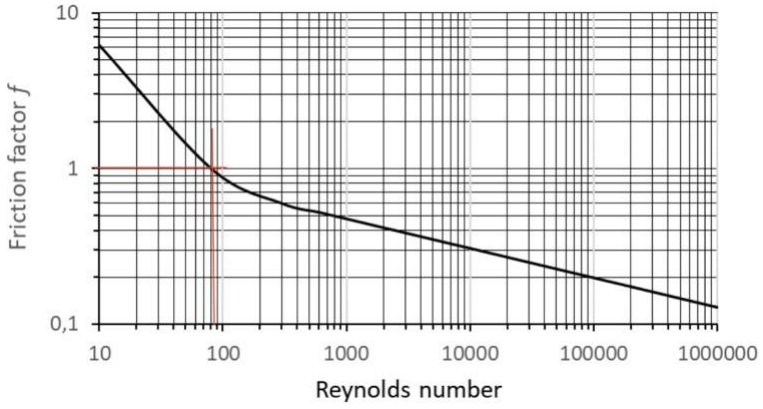

Figure 8: Correlation between Friction factor and Reynolds number.

The **concentrated pressure drops** are:

$$-\Delta p_{conc} = -4 \cdot ((4\rho_{cond} u^2{}_k)/2)$$

$$-\Delta p_{conc} = -4 \cdot ((4 \cdot\ 989.69 \cdot (48.2)^2)/2)\ = -0.0979\ Pa$$
$$\Delta p_{conc} = 0.0979\ Pa$$

Total pressure drops. Summing both main contributions

$$-\Delta p_{tot} = -\Delta p_f + -\Delta p_{conc} = -0.361 - 0.0979\ = -0.46\ Pa\ = -4.6 \cdot 10^{-6} bar$$
$$\Delta p_{tot} = 0.46\ Pa$$

Comparison between just vapor and just liquid. Both configurations give accessible pressure gain. The pressure drop given by the only vapor model gives a higher pressure drop, but in our scenario, all vapor is condensing, so it's reasonable to assume that the actual pressure drop is lower.

Result:

The design of the horizontal shell-and-tube heat exchanger successfully meets the specified thermal duty of 43 kW, achieving complete condensation of water vapor at 60 °C and 0.010627 MPa, with heat transfer to cooling water entering at 33 °C and exiting at 42 °C. The selected configuration comprises 40 copper tubes with an outer diameter of 12.7 mm and a total length of 1.51 m per tube, arranged in a 4-pass system. Furthermore, all the calculated parameters are listed below.

S.No.	Variable	Value		Unit
		Iteration - 1	Iteration - 2	
1	Log Mean Temperature Difference (LMTD)	8.74	8.74	°C
2	Heat transfer area	4.92	2.40	m²
3	Mass flow rate of water	1.14	1.14	kg/s
4	Mass flow rate of vapor	0.02	0.018	kg/s
5	Cross-sectional area of the tube	0.0008	0.008	m²
6	Number of tubes	10	10	-
7	Number of tubes for 4 passes	40.00	40.00	-
8	Reynolds number for water	20833.54	20833.54	-
9	Prandtl number for water	4.58	4.58	-
10	Heat transfer coefficient for water	6632.40	6632.40	W/(m²·K)
11	Heat transfer coefficient for the bundle	11391.35	11500.12	W/(m²·K)
12	Overall heat transfer coefficient	2046.11	2049.60	W/(m²·K)
13	New required heat transfer area	2.40	2.40	m²
14	New length of each tube	1.51	1.51	m
15	New temperature difference	1.57	1.56	K

16	Concentrated pressure drops tube side	15233.73	Pa
17	Distributed pressure drops tube side	15720.04	Pa
18	Total pressure drops tube side	30953.77	Pa
19	Concentrated pressure drops shell side vapor	1341.59	Pa
20	Distributed pressure drops shell side vapor	3038.04	Pa
21	Total pressure drops shell side vapor	4379.62	Pa
22	Concentrated pressure drops shell side liquid	0.09787	Pa
23	Distributed pressure drops shell side liquid	0.36056	Pa
24	Total pressure drops shell side liquid	0.4	Pa

Table S: Summary of all calculated properties

Conclusion:

The project achieved a successful theoretical design of a horizontal shell-and-tube heat exchanger for condensing water vapor at 60 °C and 0.010627 MPa, transferring 43 kW of heat to cooling water. A 4-pass configuration with 40 copper tubes (Ø12.7 mm, 1.51 m length) arranged in a 30° triangular pitch was selected to balance performance, compactness, and manufacturability.

Key parameters, including the log mean temperature difference, heat transfer coefficients, and pressure drops, were calculated using standard correlations and validated against engineering guidelines. The shell-side pressure drop approaches the vacuum limit but remains within acceptable bounds, confirming the design's thermal and hydraulic feasibility.

This work highlights the effectiveness of combining thermodynamic principles with analytical design methods, offering a reliable solution suitable for further optimization or experimental validation.

References:

[1]. L. Rossetto, A. Cavallini, S. Bortolin, A. Diani, Heat Transfer and Thermofluidic Dynamics, Universit`a di Padova, 2022.

[2] NIST. (2023). REFPROP—Reference Fluid Thermodynamic and Transport Properties Database. National Institute of Standards and Technology. https://www.nist.gov/srp/refprop

[3] Incropera, F. P., DeWitt, D. P., Bergman, T. L., & Lavine, A. S. (2007). Fundamentals of heat and mass transfer (6th ed.). John Wiley & Sons.

[4] TEMA. (2007). Standards of the Tubular Exchanger Manufacturers Association (9th ed.). Tubular Exchanger Manufacturers Association, Inc.

[5] Bonnacina, C., Buscarino, A., & Andreoni, B. (1980). Trasmissione del calore. [Heat transmission]. Tamburi.

[6] Kern, D. Q. (1950). Process heat transfer. McGraw-Hill.

[7] Nusselt, W. (1916). Die Oberflächenkondensation des Wasserdampfes. Zeitschrift des Vereins deutscher Ingenieure, 60(27), 541–546.

Appendices.

Appendix 1: Estimated values of the overall heat transfer coefficient

Fluido 1	Fluido 2	specifica totale di sporcamento (2) r_m [m²K/W]	globale di scambio termico (2) K_c [W/(m²K)]
Acqua (3) (4)	Acqua	$2,6 \cdot 10^{-4}$	1400-1700
	Gas, a circa 1,5-2 bar (9)	$1,7 \cdot 10^{-4}$	80-120
	Gas, a circa 8 bar (9)	$1,7 \cdot 10^{-4}$	170-230
	Gas, a circa 70 bar (9)	$1,7 \cdot 10^{-4}$	340-570
	Liquidi organici leggeri (5)	$2,6 \cdot 10^{-4}$	700-1000
	Liquidi organici medi (6)	$3,5 \cdot 10^{-4}$	420-700
	Liquidi organici pesanti (7)	$4,4 \cdot 10^{-4}$	230-420
	Liquidi organici molto pesanti (8):		
	– in riscaldamento	$7 \cdot 10^{-4}$	60-230
	– in raffreddamento	$7 \cdot 10^{-4}$	30-80
Vapor d'acqua (in condensazione)	Gas, a circa 1,5-2 bar (9)	$9 \cdot 10^{-5}$	80-120
	Gas, a circa 8 bar (9)	$9 \cdot 10^{-5}$	200-250
	Gas, a circa 70 bar (9)	$9 \cdot 10^{-5}$	400-620
	Liquidi organici leggeri (5)	$1,7 \cdot 10^{-4}$	770-1100
	Liquidi organici medi (6)	$2,6 \cdot 10^{-4}$	450-770
	Liquidi organici pesanti (7)	$3,5 \cdot 10^{-4}$	250-450
	Liquidi organici molto pesanti (8)	$6 \cdot 10^{-4}$	80-260
Id.-senza incondensabili	Acqua	$1,7 \cdot 10^{-4}$	1700-2300
Liquidi organici leggeri (5)	Liquidi organici leggeri (5)	$3,5 \cdot 10^{-4}$	570-750
	Liquidi organici medi (6)	$4,4 \cdot 10^{-4}$	400-570
	Liquidi organici pesanti (7):		
	– in riscaldamento	$5,3 \cdot 10^{-4}$	230-420
	– in raffreddamento	$5,3 \cdot 10^{-4}$	140-280
	Liquidi organici molto pesanti (8):		
	– in riscaldamento	$7 \cdot 10^{-4}$	110-280
	– in raffreddamento	$7 \cdot 10^{-4}$	30-140
Liquidi organici medi (6)	Liquidi organici medi (6)	$5,3 \cdot 10^{-4}$	280-450
	Liquidi organici pesanti (7):		
	– in riscaldamento	$6,2 \cdot 10^{-4}$	170-280
	– in raffreddamento	$6,2 \cdot 10^{-4}$	80-200
	Liquidi organici molto pesanti (8):		
	– in riscaldamento	$8 \cdot 10^{-4}$	80-170
	– in raffreddamento	$8 \cdot 10^{-4}$	30-140
Liquidi organici pesanti (7)	Liquidi organici pesanti (7)	$9 \cdot 10^{-4}$	50-170
	Liquidi organici molto pesanti (8)	$11 \cdot 10^{-4}$	30-80
Gas, a circa 1,5-2 bar (9)	Gas, a circa 1,5-2 bar (9)	0	50-90
	Gas, a circa 8 bar (9)	0	80-110
	Gas, a circa 70 bar (9)	0	90-140
Gas, a circa 8 bar (9)	Gas, a circa 8 bar (9)	0	110-170
	Gas, a circa 70 bar (9)	0	140-200
Gas, a circa 70 bar (9)	Gas, a circa 70 bar (9)	0	200-340
Acqua	Vapore organico leggero in condensazione (componente puro) (5) (10)	$1,7 \cdot 10^{-4}$	850-1100
	Vapore organico medio in condensazione (componente puro) (6) (10)	$1,7 \cdot 10^{-4}$	550-850
	Vapore organico pesante in condensazione (componente puro) (7) (10)	$3,5 \cdot 10^{-4}$	420-570

Appendix 2: Anglo-Saxon standard (Estimated external diameter and thickness)

Outside diameter (in)	Outside diameter (mm)	Wall thickness (mm)	Outside diameter (in)	Outside diameter (mm)	Wall thickness (mm)
0.25	6.35	0.711	0.875	22.225	2.108
		0.559			1.651
0.375	9.525	1.245			1.245
		0.889			0.889
		0.711	1.0	25.4	2.769
0.5	12.7	1.245			2.108
		0.889			1.651
0.625	15.875	1.651			1.245
		1.245			
		0.889	1.25	31.75	3.404
					2.769
0.75	19.05	2.769			2.108
		2.108			1.651
		1.651			
		1.245	2.0	50.08	2.769
		0.889			2.108